Electrochemical and Solid-State Letters, **12** (12) F46-F49 (2009)
1099-0062/2009/12(12)/F46/4/$25.00 © The Electrochemical Society

A Study on the Modification of Conventional Electrochemical Crystallization under Sonication: The Phenomena of Secondary Nucleation

A. Mallik,[z] A. Bankoti, and B. C. Ray

Department of Metallurgical and Materials Engineering, National Institute of Technology, Rourkela 769008, India

An understanding of the nucleation mechanism involved in the sonoelectrochemical synthesis of copper from sulfate bath is reported here. These explanations include the analysis of sono-chronoamperometric current transients and atomic force microscopy. The results indicate that ultrasound induces secondary nucleation by breakage of the existing primary nuclei in addition to the primary nucleation. The understanding of the sonoelectrochemical mechanisms clarifies a few unclear issues. It could possibly allow for the better design of sonoelectrochemical synthesis.
 [DOI: 10.1149/1.3243916]

Manuscript submitted May 18, 2009; revised manuscript received August 23, 2009. Published October 13, 2009.

Cavitation, the irradiation of liquid with high intensity ultrasound, as a means of altering the crystallization process has been reported for many systems.[1,2] It is at the solid–liquid interface that electrochemical techniques may be employed to detect the possible influence of sonication on electrochemical nucleation and growth of clusters. Cluster formation of N ions, however, is connected initially with an increase in the Gibbs energy of the system and proceeds as an energy fluctuation system expression[3-5]

$$\Delta G(N) = -N\Delta\mu + \varnothing(N) \quad [1]$$

Both the terms are functions of the size of the cluster N. The first term is associated with the degree of supersaturation, the state of unstable equilibrium, and the second term takes into consideration the total energy excess due to the creation of interfaces when a nucleus appears on the electrode surface. Thus, the interrelation between the supersaturation ($\Delta\mu$) and the size of the critical nucleus (N_{crit}) decides the lowest Gibbs energy of the phase formation (ΔG_{crit}) and the highest rate $[J = A_j \exp(-\Delta G_{crit}/BT)]$ of cluster formation. Different approaches have been established for the estimation of the parameters depending upon the size of the clusters. If adsorption, diffusion, and binding of the clusters are not the limiting factors (for sufficiently large clusters), then ΔG_{crit} has a value of

$$\Delta G_{crit} = \frac{\Delta\mu N_{crit}}{\gamma - 1} = \frac{1}{\gamma}\varphi X(N_{crit}) = \frac{1}{\gamma}\varnothing(N_{crit}) \quad [2]$$

Small crystals with a dominant effect of binding energies of adatom with substrate as well as bulk phase may have an expression for ΔG_{crit}

$$\Delta G_{crit} = \Delta\mu(N_{crit} + \beta^*) - \sum \psi_i - N_{crit}(\psi_{kink} + \varepsilon) \quad [3]$$

Hence, irrespective of the size of the initial critical nuclei, the increase in supersaturation explicitly follows a decreasing N_{crit} trend. Ultrasound capable of creating zones of extremely high level localized supersaturation[6] should set off the nucleation process. In the process of growth, however, high indexed surface zones are transformed into atomically smooth equilibrium faces. Further phase formation needs the formation of steps or irregularities on the substrate's surface for nucleation. Crystal fragmentation by ultrasound may create new steps on the defect-free crystal face to further supplement the crystallization process. Though a limited literature exists on the aspects of ultrasound-induced secondary nucleation, there is an urgent need for information particularly related to electrochemical phenomena. Thus, ultrasonic energy is believed to stimulate a biphasic nucleation sequence, i.e., primary (on the native substrate) and secondary (on the existing primary clusters).[1,2]

[z] E-mail: archananitrkl@gmail.com

The purpose of this article is to investigate the impact of ultrasound on the nucleation phenomena. The study specifically emphasizes the impact of ultrasound on the nucleation and crystal breakage. Researchers have employed fast linear sweep voltammetry and cyclic voltammetry[7,8] to observe the quantitative mass transport transient events. The methods introduce potential-driven supersaturation, and hence there may not be an effortless clear prediction of the effects. However, little attention has been paid to sonoelectrochemically modified time-dependent current analysis. An attempt has been made here to experiment the above effects through sono-chronoamperometric current transient (SCCT).

Experiments were performed on O_2-free brass substrates of an exposed surface with an area of 0.25 cm^2. The bath composition was 6.35 g L^{-1} $CuSO_4 \cdot 5H_2O$ + 60 g L^{-1} H_2SO_4. A 5 cm long platinum rod of 0.2 cm diameter and Ag/AgCl electrode (Eco Chemie, Netherlands) served as the counter and reference electrodes, respectively. Ultrasound irradiation was accomplished by a 20 kHz ultrasonic horn with a 20% output power transducer system (Sonics & Materials, VCF1500) fitted with a titanium tip. The tip was placed at a distance of 5 mm from the brass substrate. Electrochemical measurements were conducted using a potentiostat/galvanostat (Eco Chemie Netherlands, Autolab PGSTAT 12) having a computer interface of GPES software. A potential of −0.45 V (100 mV more than the estimated Nernst equilibrium potential: −0.35 V) was selected for the deposition. Experimentation was carried out for a set of time periods: 5, 10, 15, and 20 s. The current transients were fitted to an Scharifker and Hills model[9] for the determination of standard kinetics parameters, D (diffusion coefficient) and N_0 (active nucleation density). A surface morphology comparison was obtained using an SPMLab-programmed Veeco diInnova atomic force microscope (AFM) in the contact mode with a conducting p(n)-doped silicon tip.

The sonicated chronoamperometric current transients (CCTs), after a two-point Golay–Savitzky normalization, and superimposed on the original transients, are shown in Fig. 1a. The results disagree with the reports for cobalt deposition on a glassy carbon electrode.[10] All the SCCTs have a sharp initial decrease in current followed by irregular troughs and crests such as current responses. The early fall is due to the double-layer charging at the electrode surface. The rest current progression may not be inferred as noise (2 s persistence). If it was the sole impact of sonication toward truncation in diffusion spheres, then the rising current should have a decreasing tail after a higher and also sharper current peak at the maximum compared to the virgin CCT. Thus, we did interpret these irregularities as a sequence of nucleation loops. The SCCTs have the initial loop at around 1.5 s, and the successive loops abounded with the same time occurrence. The preliminary loops may be due to the conventional three-dimensional (3D) nucleation and growth. The progressive loops should support the hypothesis of secondary nucleation by crystal breakage.[1,2] The experiment has also been extended without an ultrasonic transient environment for evolving the differential

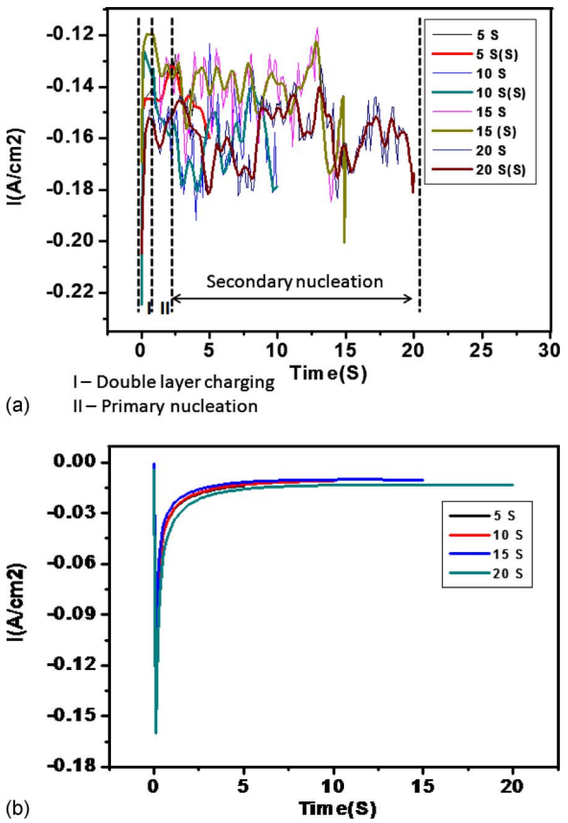

Figure 1. (Color online) CCTs for Cu deposits for different time periods. (a) Sonication and (b) silent.

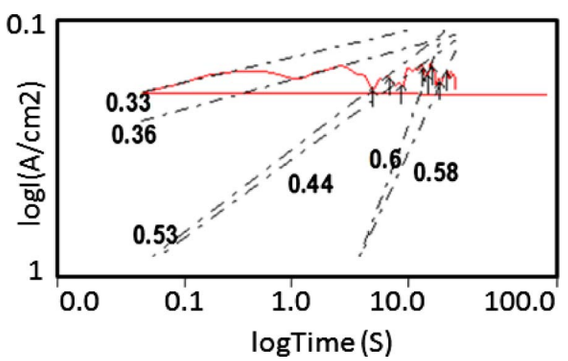

Figure 2. (Color online) Log(current density) vs log(time) plot for sonicated Cu electrodeposition at −0.45 V for 20 s.

crystal breakage. Figure 1b shows the set of recorded virgin current transients with a typical single-current maximum. The silent CCT differs from the SCCT following a typical transient of the rising portion and then a decaying current obeying the Cottrell law. The kinetics parameters were calculated using Scharfiker's[9] general equation for instantaneous nucleation

$$I_{3D}(t) = \frac{zFD^{0.5}c}{\pi^{0.5}t^{0.5}}[1 - \exp(-N_0\pi kDt)] \quad [4]$$

The slope of log(current density) vs log(time) varied from 0.3 to 0.6, which indicates instantaneous phase appearance (as shown in Fig. 2). Table I shows characteristic kinetics parameters along with total charge involved in the deposition process under insonation. The total charge consumed varies from 0.18 to 0.79 C as compared to the charges, 0.03–0.1 C, involved in the deposition without sonication. The difference may be attributed to the nucleation phenomena, as explained later. The table also contains the nuclei number density calculated for the secondary nucleation, $N_{0(S)}$, following the same model. The diffusion coefficient calculated in the silent condition was $4.2–3.2 \times 10^{-5}$ cm^2 s^{-1} compared with the values of $0.8–1.5 \times 10^{-5}$ cm^2 s^{-1} published elsewhere,[11,12] while in the presence of ultrasound the diffusion coefficient increased in values, $5.2–6.3 \times 10^{-4}$ cm^2 s^{-1}. The calculated nuclei number density for primary nucleation, $N_{0(P)}$, for all the time periods is approximately the same. The number density for the secondary nucleation increases with increasing time period, i.e., $1.8–6.06 \times 10^3$ cm^{-2}. However, the rate of increase in the number of secondary nuclei decreases with time. This may be explained by the fact that due to degassing at the electrodes, deposits are highly adherent under insonation.[2] Thus, the process of crystal breakage may not be possible for further protracted sonication.

AFM micrographs for both conditions are shown in Fig. 3 and 4 for 5, 10, 15, and 20 s. A total analysis of the area and volumetric analysis is given in Table II. Deposition without the application of ultrasound has produced coarse grains, following the conventional trend of growth of the nuclei, at longer time periods. The average height and roughness of the deposits also increase simultaneously, whereas the grains of the sonicated films become finer for extended time periods. As the time of deposition increases, the standard deviation of the grain distribution becomes narrow and smooth. The deposit at 20 s is the finest. Most of the grains fall in the height range of 10–30 nm with an average height of 24 nm. The deposit is also the smoothest, having a roughness factor of 8 nm compared to the 172 nm value of its silent counterpart. This result can be interpreted as in the following ways: Ultrasound capable of crystal breakage produces smaller grains and balances the heights of grains. This, as a result, smoothens the surfaces at a longer period of deposition. The peak and valley method of AFM analysis has been used to measure the thickness of the films (not shown). The micrograph, along with the line analysis, also shows a nearly smooth and uniform deposit under sonication. The films are mostly irregular and are far from thickness measurements through AFM line analysis for the

Table I. Characteristic kinetics parameters of $i(t)$ transients obtained for sonicated Cu deposits for different deposition time periods.

Time (s)	I_{max} (A/cm^2)	t_{max} (s)	$D \times 10^{-4}$ (cm^2 s^{-1})	$N_{0(P)} \times 10^3$ (cm^{-2})	$N_{0(S)} \times 10^3$ (cm^{-2})	$N_{0\ (T)} \times 10^3$ (cm^{-2})	Q_{total} (C)
5	0.146	1.5	5.2	3.82	1.85	5.67	0.18
10	0.150	1.7	6.3	2.78	4.42	7.2	0.397
15	0.149	1.5	5.3	3.25	5.75	9	0.531
20	0.164	1.4	6.2	3.4	6.06	9.46	0.791

Electrolyte media: 6.35 g L^{-1} $CuSO_4 \cdot 5\ H_2O$ + 60 g L^{-1} H_2SO_4. Deposition potential: −0.45 V.

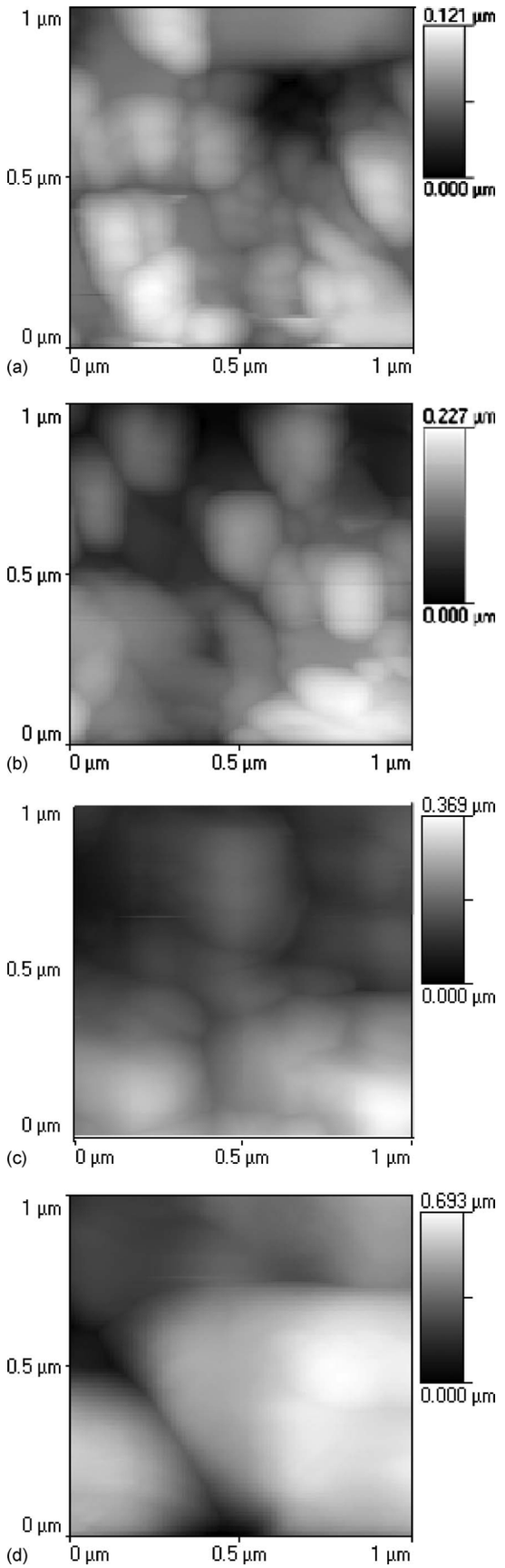

Figure 3. AFM micrographs of silent Cu deposits for (a) 5, (b) 10, (c) 15, and (d) 20 s.

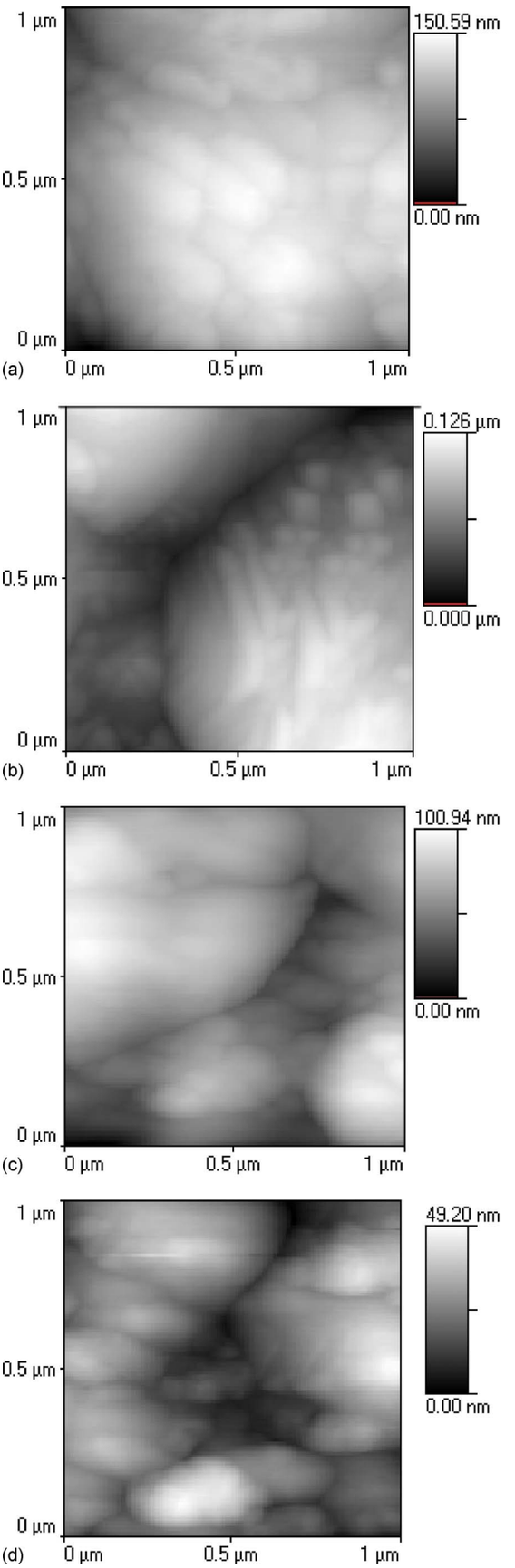

Figure 4. (Color online) AFM micrographs of sonicated Cu deposits for (a) 5, (b) 10, (c) 15, and (d) 20 s.

Table II. Roughness factor and grain size distributions from AFM measurements.

Time (s)	Roughness factor (nm)		Average height (nm)		Thickness (nm)	
	Silent	Sonication	Silent	Sonication	Calculated[a]	Measured
5	17	25	72	108	250	241
10	39	20	107	65	550	546
15	65	16	165	58	740	742
20	172	8	340	24	1100	1009

[a] Refer to the Appendix.

virgin deposits. Thus, the measured and calculated values of the nearly uniform and smooth sonicated deposits are included in Table II.

The sonication possibly imparts the ambience for promoting secondary nucleation by breaking the primary nuclei. The CCT diagram is a clear indicator of the presence of secondary nucleation phenomena. A comparison with the Scharifker and Hills limiting cases indicates that at a longer period of deposition, a crystal breakage leads to a higher population density. However, the proposed phenomenon may not proceed for an infinite period of time due to increased adherence under sonication. Contact-mode AFM has been used to confirm the conclusions drawn from the CCTs. The observed microstructural morphology is in close proximity with an anticipated reduced grain size. In contrast, the deposits without sonication consist of coarse grains. The significance of the present investigation could possibly be an understanding of the sonoelectrochemical synthesis, and following that, its use in various critical and potential applications may be opened up.

Acknowledgment

The authors thank the National Institute of Technology (NIT) for providing the necessary financial and infrastructural support.

National Institute of Technology assisted in meeting the publication costs of this article.

Appendix

The procedure for the determination of the thickness of the deposits can be presented in the following way: The calculation is based on Faraday's law; "in electrolysis, 96500 Coulombs of electric charge produce chemical charge of 1 g equivalent." If the thickness is d (cm) and the sample has an area A (cm^2), the quantity of electricity passed is Q (C), and M is the atomic mass (gm) with a density of ρ (gm cm^{-3}), then the thickness of the materials deposited can be calculated as

$$d = \frac{QM}{96{,}500nA\rho} \qquad \text{[A-1]}$$

where n represents the number of electrons involved in the reduction of the ion.

List of Symbols

A_j	constant of proportionality
B	Boltzmann constant
C	bulk concentration of electroactive species
D	diffusion coefficient
E	internal strain
F	Faraday constant
K	$(8\pi CM/\rho)^{0.5}$ (dimensionless)
M	molar mass of electroactive species
N	cluster dimensionality (1, 2, or 3)
N_0	number density of active sites
P	density of electrodeposit
t	time
T	absolute temperature
$X(N_{crit})$	extension of excess free energy of creation
Z	electrons involved

Greek

β^*	charge-transfer coefficient (dimensionless)
$\varnothing(N)$	excess free energy of creation
$\varnothing(N_{crit})$	excess free energy of creation of critical nuclei
$\Sigma\psi_i$	total binding energy of the cluster with the substrate
φ	specific boundary energy
Ψ_{kink}	binding energy of a kink atom

References

1. R. Chow, R. Blindt, R. Chivers, and M. Povey, *Ultrasonics*, **43**, 227 (2005).
2. A. Mallik and B. C. Ray, *Thin Solid Films*, In press. [DOI: 10.1016/j.tsf.2009.04.054]
3. E. Budevski, G. Staikov, and W. J. Lorenz, *Electrochim. Acta*, **45**, 2559 (2000).
4. I. V. Morkov, *Crystal Growth for Beginners*, World Scientific, Singapore (2003).
5. G. Staikov and A. Milchev, in *Electrocrystallization in Nanotechnology*, G. Staikov, Editor, Wiley-VCH, Weinheim (2007).
6. J. P. Lorimer and T. J. Mason, *Applied Sonochemistry: Uses of Power Ultrasound in Chemistry and Processing*, Wiley-VCH, Weinheim (2002).
7. G. S. Garbellini, G. R. Salzar-Banda, and L. A. Avaca, *Food Chem.*, **116**, 1029 (2009).
8. C. Agra-Gutierrez, J. L. Hardcastle, J. C. Ball, and R. G. Compton, *Analyst*, **124**, 1053 (1999).
9. B. Scharifker and G. Hills, *Electrochim. Acta*, **28**, 879 (1983).
10. S. Floate, M. Hyde, and R. G. Compton, *J. Electroanal. Chem.*, **523**, 49 (2002).
11. D. Grujicic and B. Pesic, *Electrochim. Acta*, **47**, 2901 (2002).
12. O. Ghodbane, L. Roue, and D. Belanger, *Electrochim. Acta*, **52**, 5843 (2007).